



## Synoptic-scale precipitation events recorded by high-resolution intra-shell $\delta^{18}\text{O}$ of land snail in the Asian monsoon marginal zone

Qian Zhang<sup>a,f</sup>, Jibao Dong<sup>a,\*\*</sup>, Guozhen Wang<sup>a</sup>, Fan Luo<sup>c</sup>, Ya-na Jia<sup>b</sup>, Chengcheng Liu<sup>a,c</sup>, Xiulan Zong<sup>a</sup>, Xiangzhong Li<sup>d</sup>, John Dodson<sup>a,e</sup>, Hong Yan<sup>a,b,\*</sup>

<sup>a</sup> State Key Laboratory of Loess Science, Institute of Earth Environment, Chinese Academy of Sciences, Xi'an, 710061, China

<sup>b</sup> Institute of Global Environmental Change, Xi'an Jiaotong University, Xi'an, 710049, China

<sup>c</sup> Xi'an Institute for Innovative Earth Environment Research, Xi'an, 710061, China

<sup>d</sup> Yunnan Key Laboratory of Earth System Science, Yunnan University, Kunming, 650500, China

<sup>e</sup> School of Biological, Earth and Environmental Sciences, University of New South Wales, Sydney, 2052, Australia

<sup>f</sup> University of Chinese Academy of Sciences, Beijing, 100049, China

### ARTICLE INFO

Handling Editor: Dr Mira Matthews

**Keywords:**

Land snail shell  
Oxygen isotope  
Monsoon marginal zone  
Precipitation events  
Paleoweather

### ABSTRACT

Synoptic-scale precipitation events significantly impact ecosystems and human livelihoods, and it would greatly improve our understanding of their mechanisms, if the daily scale precipitation events could be reconstructed for different climatic types in the geological past. Ultra-high resolution snail shell  $\delta^{18}\text{O}$  ( $\delta^{18}\text{O}_{\text{shell}}$ ) records obtained by secondary ion mass spectroscopy shed light on reconstructing terrestrial synoptic-scale precipitation events. However, this kind of investigation is limited due to the access and costliness of this instrumentation. In this study, we tried to reconstruct weather-scale (daily-weekly) precipitation using manually obtained intra-shell samples from living land snails (*Cathaica fasciola*) collected in northwest China in June, September, and December 2021. These shells were drilled continuously with a spatial resolution of  $\sim 500\text{--}800\ \mu\text{m}$  for isotope ratio mass spectrometer (IRMS) analysis of the  $\delta^{18}\text{O}_{\text{shell}}$ . The  $\delta^{18}\text{O}_{\text{shell}}$  profiles among individuals demonstrate satisfactory reproducibility, and notably, the reconstructed synoptic-scale precipitation frequency from the high-resolution intra-shell  $\delta^{18}\text{O}_{\text{shell}}$  is consistent with the instrumental record. This indicates that land snails  $\delta^{18}\text{O}_{\text{shell}}$  in the Asian monsoon marginal regions can be used to reconstruct daily-scale precipitation events through IRMS analysis. We speculate that snails adjust their growth strategies to accommodate the challenging environment in the arid and semi-arid regions by growing faster in the limited time of growing season when precipitation occurs. Altogether, this finding will promote the applications for reconstructing terrestrial paleoweather events.

### 1. Introduction

Synoptic fluctuations in precipitation and temperature could significantly impact ecosystems and human livelihoods. For example, typhoons, rainstorms, and heatwaves can cause great damage to environments, economies, and even human lives (Añel et al., 2017; Lesk et al., 2016; Meehl et al., 2000; Ummenhofer and Meehl, 2017). Several studies have shown that precipitation in arid and semi-arid regions (such as in monsoon marginal zones) has become more extreme in the context of continued global warming (Chen et al., 2014; Donat et al., 2016, 2019; Lehmann et al., 2015; Trenberth, 1999). Nevertheless, our knowledge about the mechanism and dynamics of extreme weather is

limited, partly due to the short timespan of modern instrumental data (generally less than 200 years). It would greatly improve our understanding of their mechanisms, if they could be reconstructed for different climatic types in the geological past. Paleoclimate archives could serve as an important supplement for this purpose, which has been widely used to investigate climate change in the past (e.g., An et al., 2011; Cook et al., 2010; Cheng et al., 2016; Liu and Ding, 1998; Zachos et al., 2001). However, the temporal resolution of most terrestrial archives is generally low-resolution (monthly at most), and thus, it's still difficult to study synoptic-scale variations.

Land snails are gastropods, with rich species numbers and wide distributions (Barker, 2001). They are regarded as "indicator animals" in

\* Corresponding author. State Key Laboratory of Loess Science, Institute of Earth Environment, Chinese Academy of Sciences, Xi'an 710061, China.

\*\* Corresponding author.

E-mail addresses: [djb@ieecas.cn](mailto:djb@ieecas.cn) (J. Dong), [yanhong@ieecas.cn](mailto:yanhong@ieecas.cn) (H. Yan).

studying the climate changes recorded in loess deposits (Liu, 1985), and are one of the key proxies for paleoclimate reconstructions (e.g., Abell and Plug, 2000; Colonese et al., 2010; Goodfriend, 1992; Rech et al., 2021; Wang et al., 2016; Wu et al., 2018; Yanes et al., 2019). In early studies, fossil snail species' assemblages were often used to investigate climatic and environmental changes (e.g., Li et al., 2008; Rousseau and Wu, 1997; Wu et al., 1998, 2001, 2018). Meanwhile, some researchers explored the  $\delta^{18}\text{O}$  of snail shell ( $\delta^{18}\text{O}_{\text{shell}}$ ) using isotope ratio mass spectrometer (IRMS) to reconstruct climatic and environmental changes (e.g., Kehrwald et al., 2010; Léolle, 1985; Magaritz and Heller, 1980; Prendergast et al., 2015; Yapp, 1979; Zanchetta et al., 2005). According to the flux balance model of Balakrishnan and Yapp (2004), the  $\delta^{18}\text{O}_{\text{shell}}$  is influenced by several environmental variables, including temperature, RH, the  $\delta^{18}\text{O}$  of liquid water ingested by the snail, and  $\delta^{18}\text{O}$  of ambient water vapor. Recent studies have shown that the  $\delta^{18}\text{O}_{\text{shell}}$  is determined largely by the  $\delta^{18}\text{O}$  of precipitation, although the influence of temperature and RH should not be ignored (Yanes et al., 2018, 2019; Wang et al., 2019; Bao et al., 2019, 2020; Nield et al., 2022).

The above-mentioned studies on  $\delta^{18}\text{O}_{\text{shell}}$  mainly focused on whole-shell or multi-shells. Leng et al. (1998) were the first to conduct the high-resolution intra-shell sampling of *Limicolaria kambeul chudeaui* Germain and they indicated that the intra-shell  $\delta^{18}\text{O}_{\text{shell}}$  may reflect seasonal variations of precipitation  $\delta^{18}\text{O}$ . Subsequently, more intra-shell analyses were conducted (e.g., Dong et al., 2022; Dettman et al., 2024; Goodfriend and Ellis, 2002; Ghosh et al., 2017; Rangarajan et al., 2013; Wang et al., 2016; Wang et al., 2020; Yanes et al., 2014). For example, Ghosh et al. (2017) reconstructed the variability of the Indian summer monsoon precipitation by sampling *Lissachatina fulica* (Bowdich) at 2 mm and 4 mm intervals, which demonstrates the utility of the  $\delta^{18}\text{O}_{\text{shell}}$ .

in reconstructing precipitation on seasonal to sub-seasonal timescales. Wang et al. (2020) used the range of intra-shell  $\delta^{18}\text{O}_{\text{shell}}$  ( $\delta^{18}\text{O}_{\text{shell-max}} - \delta^{18}\text{O}_{\text{shell-min}}$ ) of *Cathaica* species from the Chinese Loess Plateau to reveal the seasonal dry and wet variability of the Asian monsoon since the middle Pleistocene. These studies indicated that the  $\delta^{18}\text{O}_{\text{shell}}$  can not only reconstruct the paleo-environment and paleo-ecological changes on orbital timescale, but also has the potential to reveal the climatic environment changes on seasonal and sub-seasonal timescales.

Recently, several studies adopted secondary ion mass spectroscopy (SIMS) to achieve ultra-high spatial resolution (at the micron level) and show that land snails can reveal climate change on synoptic-scales (Dong et al., 2022; Wang et al., 2024a). Dong et al. (2022) found that six abrupt negative fluctuations in the SIMS  $\delta^{18}\text{O}_{\text{shell}}$  of *Cathaica fasciola* (*C. fasciola*) matched well with the instrumental precipitation events, indicating that the  $\delta^{18}\text{O}_{\text{shell}}$  records have the potential to reconstruct weekly-daily precipitation events. Moreover, a super rainstorm event was quantitatively reconstructed using the ultra-high resolution  $\delta^{18}\text{O}_{\text{shell}}$  records of *C. fasciola* (Wang et al., 2024a). On these bases, Wang et al. (2025) further showed that the first derivation of SIMS  $\delta^{18}\text{O}_{\text{shell}}$  of *C. fasciola* could reconstruct the frequency of synoptic-scale precipitation events.

Thus far, however, the use of SIMS analysis for land snails for paleo-weather reconstructions will remain limited, mainly due to limited instrument availability, expensive costs, and requirements in sample preparations. Therefore, this study aims to reconstruct synoptic-scale precipitation events using intra-shell  $\delta^{18}\text{O}_{\text{shell}}$  data from IRMS analysis. Considering the high sensitivity of monsoon marginal zones to climatic and environmental changes and the well-preserved fossils in this region, live *C. fasciola* snails were collected nearby, at Shizuishan

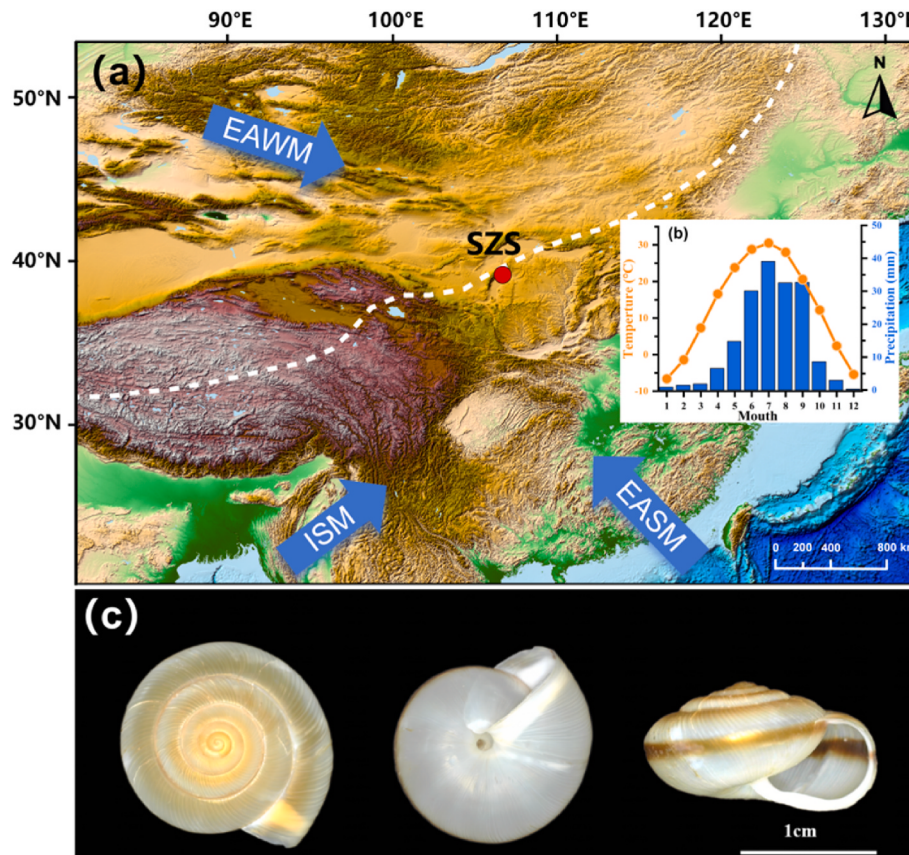


**Fig. 1.** (a) The location of the study site, Shizuishan (SZS, red dot). The white dashed line indicates the approximate margin of the modern summer Asian monsoon (Chen et al., 2015). EAWM, ISM, and EASM denote the East Asian Winter Monsoon, the Indian Summer Monsoon, and the East Asian Summer Monsoon, respectively. (b) The monthly mean temperature (yellow line) and precipitation (blue bars) at the study site from 1999 to 2020. (c) The modern *Cathaica fasciola* in apical, umbilical, and lateral views. (For interpretation of the references to colour in this figure legend, the reader is referred to the Web version of this article.)

(SZS) city (Fig. 1a), and the shells were continuously sub-sampled at ~500–800 µm intervals for IRMS analysis. This study assesses whether  $\delta^{18}\text{O}_{\text{shell}}$  signatures obtained from IRMS analysis can reconstruct weather-scale (daily-weekly) precipitation events at the northwest margin of the East Asian summer monsoon.

## 2. Materials and methods

### 2.1. Study area and sample collection

Shizuishan (SZS) city is situated within the marginal zone of the East Asian summer monsoon in northwestern China (Fig. 1a). There is a fragile ecosystem and precipitation is concentrated in summer (Fig. 1b). Modern specimens of live *C. fasciola* were collected at the SZS site (106.68°E, 39.16°N, 1056 m a.s.l.) during three sampling campaigns (June 8th, September 12th, and December 15th in 2021). The snails were non-adults according to their shell size (the number of spiral whorls) (Chen and Zhang, 2004). Snails collected in June and September were in active states, whereas those obtained in December were in an inactive state with fresh epiphramgs covering the apertures. All shells were collected in minimized potential anthropogenic or hydrological influences, including rivers, lakes, managed woodlands, and residential zones.

### 2.2. Sample preparation

In this study, the seven snails were labeled as 0608-1, 0608-2, 0912-1, 0912-2, 0912-3, 1215-1, and 1215-2 according to the sampling date (Table 1). The 0608-1, 0912-1, and 1215-1 snail samples had medium sizes (length \* width is 12.5 mm \* 10.5 mm, 13.0 mm \* 11.5 mm, and 11.0 mm \* 10.0 mm, respectively), while the others were smaller. The samples were treated as follows: (1) Remove the snail's soft tissue with a dissection needle. (2) Soak the shell in 3 % H<sub>2</sub>O<sub>2</sub> (set the pH to neutral) overnight at room temperature to remove organic components adhered to the shell, then thrice ultrasonically rinsed with deionized water. (3) Using a diamond wire-cutting machine, and the shells were divided into two parts. (4) The upper part was filled with epoxy resin. After the resin was completely solidified, it was attached to the slide. (5) Under the microscope, the intra-shell sub-samples were collected continuously using the 0.3 mm diameter dental drill. Low-speed drilling was employed to prevent potential thermal influence and obtain as many sub-samples as possible. Sampling commenced at the shell aperture, with drilling perpendicular to the growth lines along the body whorl. In total, 625 sub-samples were collected from seven snails in this study.

### 2.3. Stable isotope analysis

All the  $\delta^{18}\text{O}_{\text{shell}}$  values were determined by Delta V Advantage isotope ratio mass spectrometer coupled to the Kiel IV carbonate device. About 70 µg of carbonate powder sample was reacted at 70 °C with 3 drops of 105 % phosphoric acid (H<sub>3</sub>PO<sub>4</sub>) to produce CO<sub>2</sub>. Water and non-condensable gases were removed by a freezing device, and the purified CO<sub>2</sub> was introduced into the mass spectrometer through a

capillary for the  $\delta^{18}\text{O}$  test. Results were calibrated using laboratory standard carbonate (GBW04405) and were reported on the Vienna-Pee Dee Belemnite (V-PDB) scale, which had a composition of  $\delta^{18}\text{O} = -8.49 \pm 0.15 \text{ ‰}$  (V-PDB). Analytical precision for replicate measurements of  $\delta^{18}\text{O}$  on this standard is  $\pm 0.12 \text{ ‰}$  ( $n = 58$ ,  $1\sigma$ ).

### 2.4. Instrumental data collection

The meteorological information of Huinong Station (~8 km from the sampling site), including temperature, precipitation, and RH, were obtained from the National Meteorological Data Center (<http://data.cma.cn/>). Based on the instrument data from 1999 to 2020, the mean annual temperature is ~13 °C, ranging from -6.6 °C in January to 30.5 °C in July (Fig. 1b). The annual precipitation is about 172 mm, mainly concentrated from June to September (Fig. 1b). The mean monthly RH is ~46 %, ranging from 31 % in April to 58 % in September. The maximum RH value in the summer and fall seasons is ~87 %. In 2021, the mean annual temperature is 11.6 °C, with the minimum mean daily temperature of -17.1 °C on January 7th and a maximum of 30.2 °C on July 14th. The annual precipitation is 113.1 mm, with 34 precipitation days. The RH ranged from 13 % to 86 % and it fluctuated significantly with an abrupt rise following precipitation events. September recorded the highest RH values. Accordingly, snails are primarily active in summer and fall seasons in the studied region.

## 3. Results

The results show significant variations in  $\delta^{18}\text{O}_{\text{shell}}$  for snails collected in different periods. For the *C. fasciola* collected on June 8th, the  $\delta^{18}\text{O}_{\text{shell}}$  of 0608-1 snail and 0608-2 snail range from -5.7 to 3.0 ‰, -5.5 to 0.1 ‰, with mean values of -2.3 ‰ and -2.6 ‰, respectively (Fig. 2a, Table 1). For snails sampled on September 12th, the  $\delta^{18}\text{O}_{\text{shell}}$  varied from -5.4 to 2.1 ‰ for 0912-1 snail, from -5.7 to -2.0 ‰ for 0912-2 snail, and from -5.3 to 0.8 ‰ for sample 0912-3 snail (Fig. 2b, Table 1). The corresponding mean  $\delta^{18}\text{O}_{\text{shell}}$  of the three samples were -2.3 ‰, -4.1 ‰ and -2.5 ‰, respectively. For snails collected on December 15th, the  $\delta^{18}\text{O}_{\text{shell}}$  of 1215-1 snail and 1215-2 snail range from -6.3 to 2.2 ‰ and -5.3 to -0.6 ‰, with mean values of -2.7 ‰ and -3.0 ‰, respectively (Fig. 2c, Table 1).

## 4. Discussion

### 4.1. Verify the reproducibility of $\delta^{18}\text{O}_{\text{shell}}$

Since the individuals collected in June and September were alive and non-adult, it is reasonable to assume that the sampling dates are the formation dates for the first sampling points at the shell aperture. Thus, we aligned the  $\delta^{18}\text{O}_{\text{shell}}$  records from the snail aperture to investigate their reproducibility. This is also the method commonly adopted by previous studies (Ghosh et al., 2017; Dong et al., 2022; Li et al., 2024; Wang et al., 2024a). However, the date of the last growth band at the shell aperture is unknown for 1215-1 and 1215-2 snails, because they had ceased growing and were in dormancy at the sampling date.

**Table 1**

Information of *Cathaica fasciola* including the collection date, state of snails, sample ID, number of sub-samples, average sampling resolution, as well as the maximum, minimum, average, and amplitude of the  $\delta^{18}\text{O}_{\text{shell}}$  values ( $\Delta^{18}\text{O}$ , which is maximum minus minimum  $\delta^{18}\text{O}_{\text{shell}}$  values).

Collection date	State at sampling	Sample ID	Length*width (mm)	Number of sub-samples	Average sampling resolution(µm)	$\delta^{18}\text{O}_{\text{ave}}$ (%)	$\delta^{18}\text{O}_{\text{Max}}$ (%)	$\delta^{18}\text{O}_{\text{Min}}$ (%)	$\Delta^{18}\text{O}$ (%)
2021/6/8	active	0608-1	12.5 * 10.5	102	660	-2.3	3.0	-5.7	8.7
	active	0608-2	11.0 * 9.5	82	770	-2.6	0.1	-5.5	5.6
2021/9/12	active	0912-1	13.0 * 11.5	108	630	-2.3	2.1	-5.4	7.5
	active	0912-2	11.5 * 10.0	68	740	-4.1	-2.0	-5.7	3.7
2021/12/15	active	0912-3	11.0 * 9.5	79	790	-2.5	0.8	-5.3	6.1
	dormant	1215-1	11.0 * 10.0	96	680	-2.7	2.2	-6.3	8.5
	dormant	1215-2	10.5 * 9.0	90	530	-3.0	-0.6	-5.3	4.7

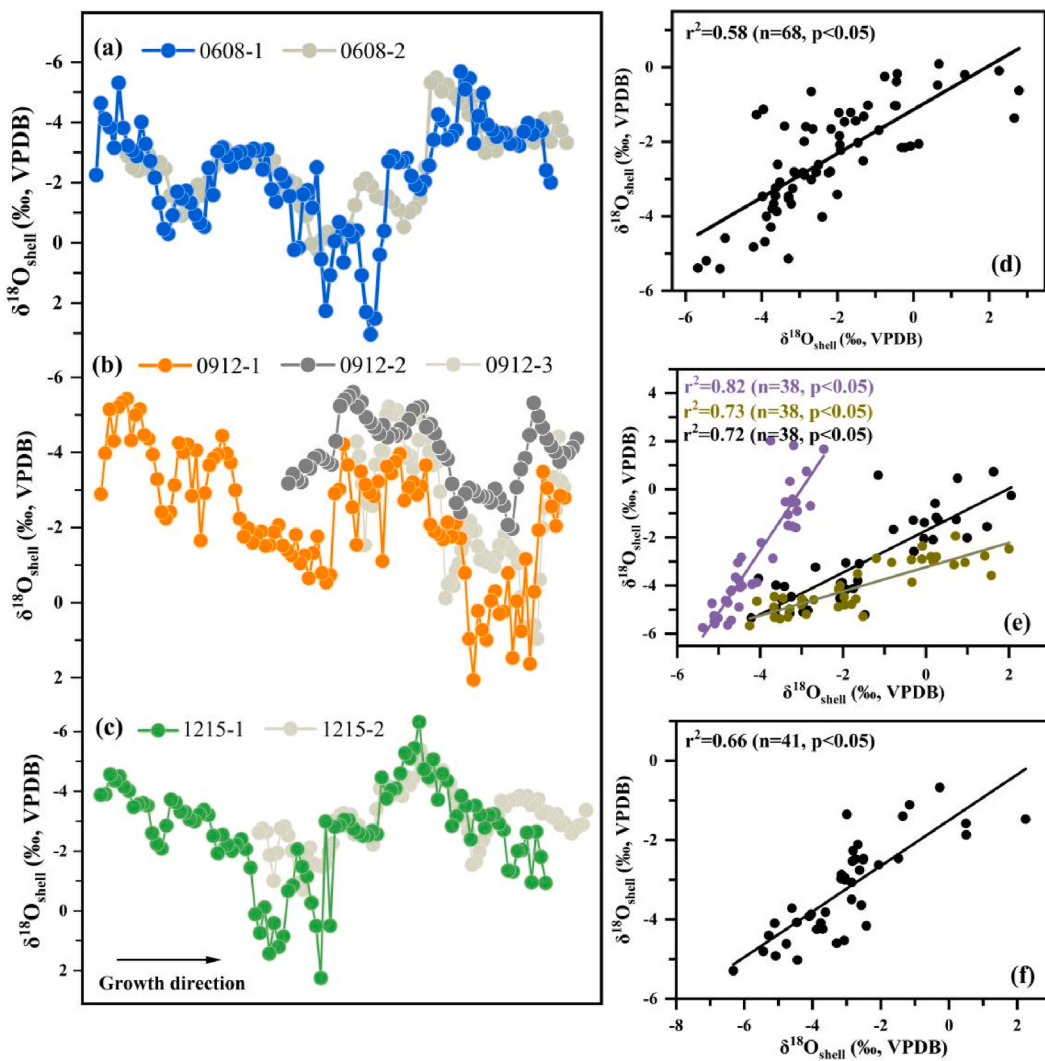


**Fig. 2.** The  $\delta^{18}\text{O}_{\text{shell}}$  profiles of *Cathaica fasciola* collected on June 8th (a;  $n = 102$  for 0608-1,  $n = 82$  for 0608-2), September 12th (b;  $n = 108$  for 0912-1,  $n = 68$  for 0912-2,  $n = 79$  for 0912-3), and December 15th (c;  $n = 96$  for 1215-1,  $n = 90$  for 1215-2) in 2021, where  $n$  is the number of sub-samples. Correlation analyses of  $\delta^{18}\text{O}_{\text{shell}}$  were performed on contemporaneous shells collected in June (d;  $r^2 = 0.58$ ,  $p < 0.05$ ), September (e), and December (f;  $r^2 = 0.66$ ,  $p < 0.05$ ). For September samples, significant correlations were observed among 0912-2 vs 0912-3 ( $r^2 = 0.82$ ,  $p < 0.05$ ), 0912-1 vs 0912-2 ( $r^2 = 0.72$ ,  $p < 0.05$ ), and 0912-1 vs 0912-3 ( $r^2 = 0.73$ ,  $p < 0.05$ ). The black arrow indicates the growth direction of the snails. The X-axis is not shown for clarity, which is the sequential number of sub-samples (i.e., 1, 2, 3 ...) from the aperture at the rightmost to the apex.

As shown in Fig. 2, the intra-shell  $\delta^{18}\text{O}_{\text{shell}}$  profiles of snails collected in June almost overlap with each other (Fig. 2a), and they show similar variations for the snails collected in September although the absolute  $\delta^{18}\text{O}_{\text{shell}}$  values and the profile lengths of time vary (Fig. 2b). The snails collected in December may have dormancy at different dates. Still, their intra-shell  $\delta^{18}\text{O}_{\text{shell}}$  profiles are also comparable (Fig. 2c). To quantitatively assess reproducibility, we performed Pearson correlation analyses for the overlapping parts of the  $\delta^{18}\text{O}_{\text{shell}}$  data (Figs. S1–S3 in Supplementary Information), which were potentially formed in the same period. The results showed strong correlations ( $r^2 = 0.58\text{--}0.82$ ,  $p < 0.05$ ) among different individuals (Fig. 2d–f). The high correlations of  $\delta^{18}\text{O}_{\text{shell}}$  records among different snails demonstrate that inter-individual differences were not significant.

Notably, the lowest  $\delta^{18}\text{O}_{\text{shell}}$  value for different individuals collected at the same period is very similar. For instance, the lowest values for 0608-1 snail and 0608-2 snail are  $-5.7\text{ ‰}$  and  $-5.5\text{ ‰}$ , respectively (Fig. 2a). However, the highest  $\delta^{18}\text{O}_{\text{shell}}$  values differ markedly. In particular, the highest  $\delta^{18}\text{O}_{\text{shell}}$  values for three snails collected in September were  $2.1\text{ ‰}$ ,  $-2.0\text{ ‰}$ , and  $0.8\text{ ‰}$ , respectively (Fig. 2b). In addition, it seems that the larger-size snails have higher  $\delta^{18}\text{O}_{\text{shell}}$  values.

We observed that the highest  $\delta^{18}\text{O}_{\text{shell}}$  values for the larger snails 0608-1 (12.5 mm \* 10.5 mm), 0912-1 (13.0 mm \* 11.5 mm), 1215-1 (11.0 mm \* 10.0 mm) are higher than those for the smaller snails 0608-2 (11.0 mm \* 9.5 mm), 0912-2 (11.5 mm \* 10.0 mm) and 0912-3 (11.0 mm \* 9.5 mm), 1215-2 (10.5 mm \* 9.0 mm), respectively (Table 1). These results may be primarily attributed to the physiology of snails. Generally, snails become active when precipitation occurs and the  $\delta^{18}\text{O}$  of snails' body water ( $\delta^{18}\text{O}_{\text{body water}}$ ), which is finally transferred into the snail shell, is paced by the variations of precipitation  $\delta^{18}\text{O}$  (Zong et al., 2023). Thus, snails recorded similar values for the lowest  $\delta^{18}\text{O}_{\text{shell}}$  as it is probably derived from same precipitation event. The  $\delta^{18}\text{O}_{\text{body water}}$  will become enriched until the next rainfall (Goodfriend et al., 1989; Zong et al., 2023). The enrichments of  $\delta^{18}\text{O}_{\text{body water}}$  following rainfall are probably different because of varying environmental niches for different snails. For example, smaller and younger snails may be less tolerant to drought than large snails (Rangarajan et al., 2013; Thakur and Kumari, 1998), so they prefer the more humid micro-environment. In this context, their  $\delta^{18}\text{O}_{\text{body water}}$  and  $\delta^{18}\text{O}_{\text{shell}}$  will be more negative compared with large snails.

Overall, the intra-shell  $\delta^{18}\text{O}_{\text{shell}}$  profiles of different snails show

similar patterns (Fig. 2a–c), although there are differences in the absolute  $\delta^{18}\text{O}_{\text{shell}}$  values. The natural conditions in the studied region (e.g., temperature, precipitation, and RH) may mainly contribute to this good repeatability, because the warm and humid conditions are limited to the summer season, which may restrict the snail's activity and shell growth to relatively limited intervals.

#### 4.2. Establish the age framework of $\delta^{18}\text{O}_{\text{shell}}$ profiles

To investigate the potential of the intra-shell  $\delta^{18}\text{O}_{\text{shell}}$  response to synoptic-scale changes, it's necessary to establish the age framework for  $\delta^{18}\text{O}_{\text{shell}}$  profiles. As discussed above, the first sub-sample at the shell aperture for 0608-1 and 0912-1 snails corresponds to June 8th and September 12th, respectively. These serve as the age control points for integrating the  $\delta^{18}\text{O}_{\text{shell}}$  profiles of snails collected on different dates. We found that the  $\delta^{18}\text{O}_{\text{shell}}$  profiles of the body whorl part for 0912-1 snail mimics the variations for the apex part of 1215-1 snail (Fig. 3a), although the ceased-growing point could not be constrained for the latter one. Moreover, there are also similar variations between the body whorl part for 0608-1 snail and the apex part 0912-1 snail (Fig. 3a). In this case, we have confidence to transfer the two age-controlling points of June 8th and September 12th to the  $\delta^{18}\text{O}_{\text{shell}}$  profiles of 0912-1 snail and 1215-1 snail, respectively (Fig. 3a). Therefore, we can establish a  $\delta^{18}\text{O}_{\text{shell}}$  record from June 8th to September 12th.

To verify the reliability of the proposed time framework, we performed correlation analysis for the overlapping parts (Fig. 3b–d). Date points of the overlap parts were interpolated to the same number by the cubic spline method before the correlation analysis. The results show

that the  $\delta^{18}\text{O}_{\text{shell}}$  records are well-correlated for the overlapping segments. There is also a strong correlation when the two overlapping parts are combined (Fig. 3d). In detail, the slopes are around ~0.8, and  $r^2 = 0.36$  ( $p < 0.05$ ),  $r^2 = 0.68$  ( $p < 0.05$ ) and  $r^2 = 0.71$  ( $p < 0.05$ ), respectively (Fig. 3b–d). The correlation relationship between the aperture of the 0608-1 snail and the apex of the 0912-1 snail is relatively low, but similar fluctuations still could be observed by the naked eye (Fig. 3b). This may be attributed to the limited number of data points and the narrow range of  $\delta^{18}\text{O}_{\text{shell}}$  values. Altogether, these suggest the established chronology framework is reliable, which makes it possible to study the growth rate of snail shells and potential synoptic-scale information embedded in the intra-shell  $\delta^{18}\text{O}_{\text{shell}}$  profiles.

#### 4.3. Calculated the growth rate of snail shell

To estimate whether the temporal resolution of intra-shell samples could record synoptic-scale events under the current sampling strategy, we calculated the growth rate of snail shells between two age control points (see section 4.2). The length of 0912-1 snail shell was ~5.3 cm between June 8th and September 12th, which corresponds to 97 days. Assuming a constant growth rate, the snail's daily growth increment is ~543  $\mu\text{m}$  (Fig. 3a). Thus, our sub-samples approximately approach daily resolution, because the data was collected at ~500–800  $\mu\text{m}$  intervals. In addition, assuming the 0912-1 snail and 1215-1 snail have the same and constant growth rate, their hatching dates are estimated to be ~May 14th and July 15th, respectively. Studies suggested that the incubation of snail eggs is significantly affected by temperature and precipitation (e.g., Hong et al., 2006; Li et al., 2021). There were several precipitation

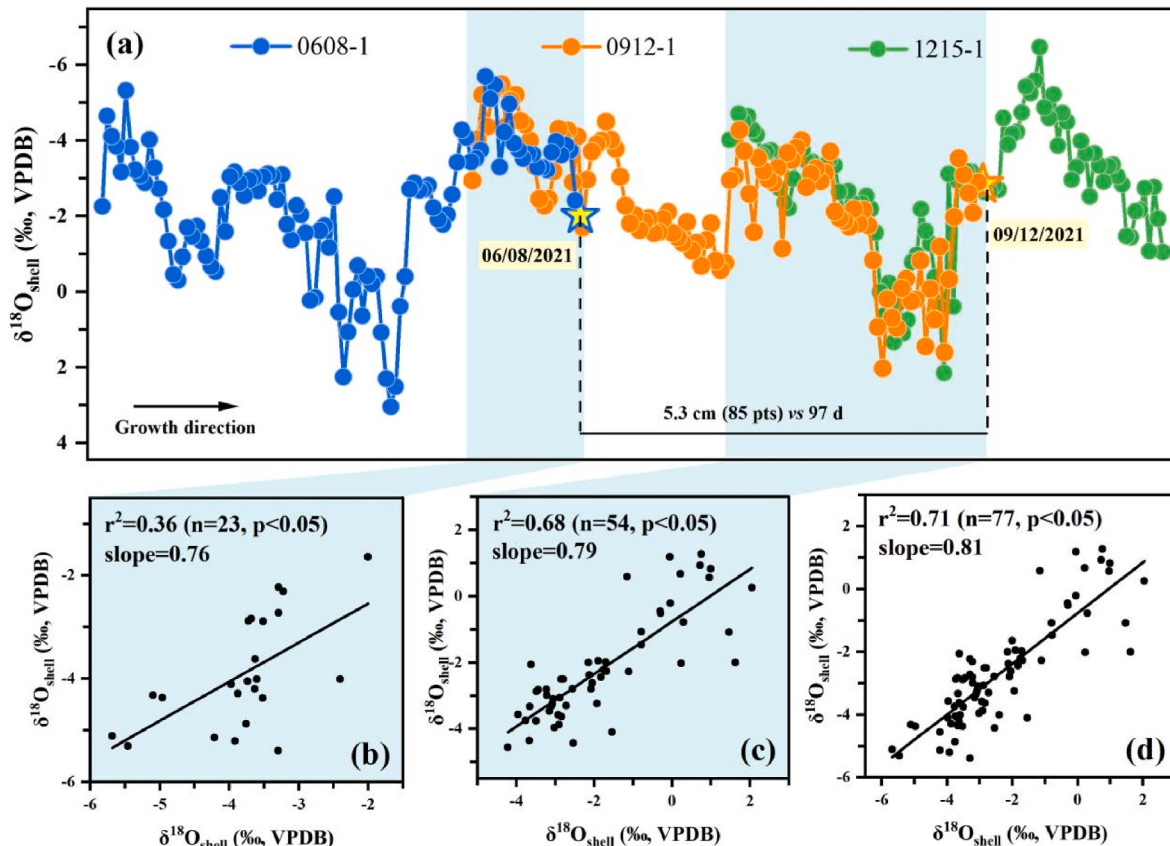


**Fig. 3.** The comparison of the  $\delta^{18}\text{O}_{\text{shell}}$  profiles of 0608-1, 0912-1 and 1215-1 snails (a) and the correlation analyses for the overlapping parts between 0608-1 and 0912-1 (b;  $r^2 = 0.36$ ,  $p < 0.05$ ), between 0912-1 and 1215-1(c;  $r^2 = 0.68$ ,  $p < 0.05$ ) and for the two sets of data (d;  $r^2 = 0.71$ ,  $p < 0.05$ ).  $n$  is the number of data points. The two yellow stars are the age control points for June 8th and September 12th in 2021, respectively. The X-axis is not shown for clarity, which is the sequential number of sub-samples (i.e., 1, 2, 3 ...) from the aperture at the rightmost to the apex. (For interpretation of the references to colour in this figure legend, the reader is referred to the Web version of this article.)

events from mid-May to late-July, and the temperature was favorable for snails during this time interval (Fig. 4a and 4d). Furthermore, the negative excursions of  $\delta^{18}\text{O}_{\text{shell}}$  values also support the occurrence of precipitation events according to previous study (Zong et al., 2023). Interestingly, the apex parts for 0608-1 snail have similar  $\delta^{18}\text{O}_{\text{shell}}$  values as 0912-1 and 1215-1 snails, suggesting possible incubation during the warm and wet season in the preceding year (Fig. 3a). Moreover, previous reports indicated that snail mating and egg laying mainly started in mid-April to mid-May when the temperature is between 13 and 25 °C (Hong et al., 2006; Mei, 2016; Xu et al., 2002), and the egg laying of snail could last to late-July when conditions are not suitable (Xu et al., 2002). These results suggest that the age frame and estimated growth rates proposed for these shells are reasonable. In brief, the growth rate of *C. fasciola* is high enough to obtain daily resolution samples manually, and thus, its  $\delta^{18}\text{O}_{\text{shell}}$  could be used to explore synoptic-scale precipitation events in the studied region.

*C. fasciola* is a common snail species in northern China and previous studies also estimated its growth rates. The first attempt suggested that it is 56 µm/day in Xi'an (Dong et al., 2022). The growth rates calculated by Wang et al. (2024a) were 73 µm/day and 259 µm/day before and after the rainstorm in Zhengzhou, respectively. Recent work showed the average growth rate was ~290 µm/day (from 250 to 330 µm/day) for non-adults (Li et al., 2024). Wang et al. (2024b) found that the growth rate of *Cathaica* sp. was faster during the late April to early August interval, and it could reach 4.6 mm/month, i.e. ~153 µm/day. The culture experiment observed that the growth rate of African giant snail *Lissachatina fulica* is  $0.40 \pm 0.28$  cm/week, that is  $571 \pm 400$  µm/day (Rangarajan et al., 2013). These studies showed that the growth rate of snails varies greatly, which may be attributed to the following: Firstly, species differences may be a primary factor and the larger snails might have a high growth rate. Second, the environmental conditions may contribute to the observed differences within the same species, e.g., temperature, precipitation, relative humidity, food availability, and external calcium sources (Oosterhoff, 1977; Rangarajan et al., 2013;

Wang et al., 2024a; Zong et al., 2023). These factors could significantly affect the snail's activities and the formation of the shell. Third, the growth rate may vary at different growth stages, e.g., juveniles versus adults (Oosterhoff, 1977; Upatham et al., 1988). Besides, discrepancies among different studies may also arise from the estimated age framework or age controlling points. In the studied arid and semi-arid regions, snail activity is mainly confined to June to September, which is much shorter compared with other warm-humid regions. Therefore, snails may accommodate the challenging environments by growing faster and achieving adulthood during the limited time with less water, considering the capacity to survive and reproduction.

#### 4.4. Reconstruct the synoptic-scale precipitation frequency by IRMS $\delta^{18}\text{O}_{\text{shell}}$

Mollusks are sensitive to environmental changes and can record fluctuations at synoptic-scale and even at hourly resolution (Dong et al., 2022; Wang et al., 2024a, 2025; Yan et al., 2020). Previous studies have demonstrated that land snail  $\delta^{18}\text{O}_{\text{shell}}$  has the potential to reflect weather-scale changes (Dong et al., 2022; Wang et al., 2024a, 2025). Based on the age framework mentioned above, we attempted to compare the  $\delta^{18}\text{O}_{\text{shell}}$  profiles with contemporaneous temperature, RH, and precipitation (Fig. 4), which are considered as key environmental factors influencing the  $\delta^{18}\text{O}_{\text{shell}}$  of land snails (e.g., Bao et al., 2019; Balakrishnan and Yapp, 2004; Liu et al., 2006; Nield et al., 2022; Wang et al., 2019). On the whole, the  $\delta^{18}\text{O}_{\text{shell}}$  profiles display three negative fluctuations from June 8th and September 12th, which corresponds to three time periods of precipitation, and two positive  $\delta^{18}\text{O}_{\text{shell}}$  intervals for dry periods (Fig. 4e and 4h). Meanwhile, the RH shows similar variations as precipitation, with high and low RH values for precipitation and dry periods, respectively (Fig. 4c), and the mean daily temperature is also favorable for snails (Fig. 4b). The fluctuations of  $\delta^{18}\text{O}_{\text{shell}}$  could therefore be explained by observed changes of snail body water  $\delta^{18}\text{O}_{\text{body}}$ , which has a large impact on the  $\delta^{18}\text{O}_{\text{shell}}$  (Zong et al., 2023). The

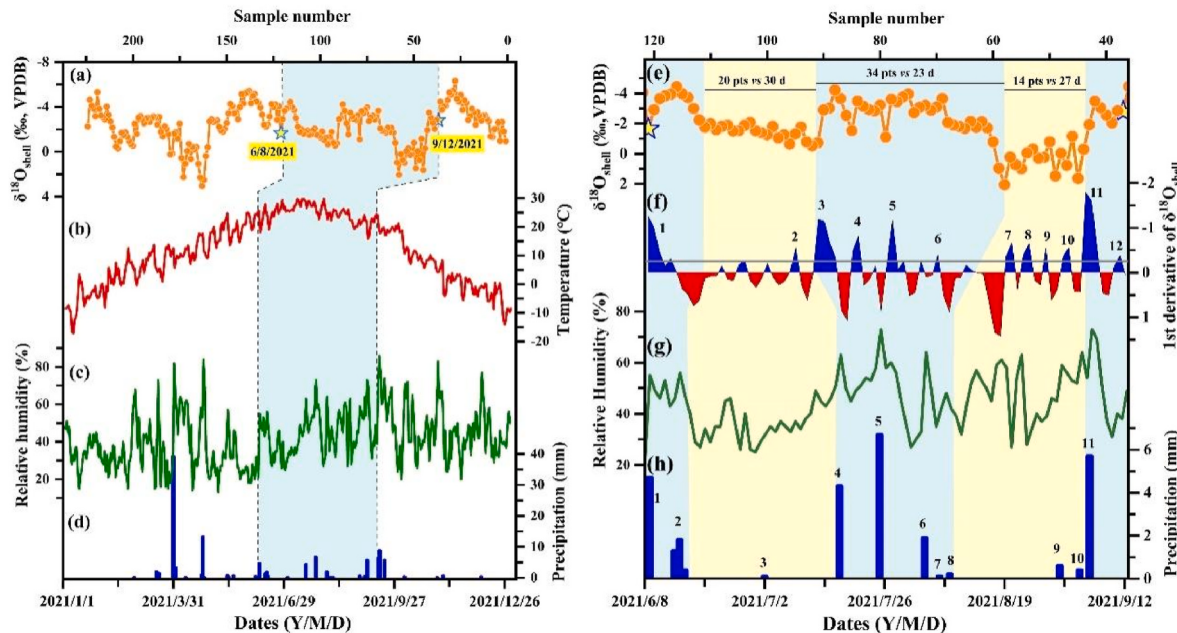


**Fig. 4.** Left: the comparison of the  $\delta^{18}\text{O}_{\text{shell}}$  on the X-axis of sample ID (a) with daily average temperature (b), relative humidity (c), and precipitation amount (d) in 2021. Right: the comparison of the  $\delta^{18}\text{O}_{\text{shell}}$  records of 0912-1 snail (e), the first derivative of  $\delta^{18}\text{O}_{\text{shell}}$  (f) with the relative humidity (c) and precipitation amount (d) from June 8th to September 12th. The horizontal gray lines indicate the 30th percentile of negative derivative values which is regarded as the threshold for identifying the significant excursions of the first derivative values (Wang et al., 2025). The numbers above the first derivative profiles and daily precipitation records denote the count of significant  $\delta^{18}\text{O}_{\text{shell}}$  negative shifts and synoptic-scale precipitation events, respectively. The two yellow stars are the age control points for June 8th and September 12th in 2021, respectively. (For interpretation of the references to colour in this figure legend, the reader is referred to the Web version of this article.)

$\delta^{18}\text{O}_{\text{body}}$  water tends to be more negative during precipitation, while it gradually becomes more positive during dry periods (Goodfriend et al., 1989; Zong et al., 2023). This is likely because the newly introduced rainwater typically exhibits more negative  $\delta^{18}\text{O}$  values than the body water, which has undergone evaporation. These synchronous variations of  $\delta^{18}\text{O}_{\text{shell}}$  and precipitation further support the reliability of the chronological framework.

Recently, a new statistical method for reconstructing synoptic-scale precipitation frequency from daily resolved SIMS  $\delta^{18}\text{O}_{\text{shell}}$  records was proposed by Wang et al. (2025). Specifically, the negative peaks in the first derivative  $\delta^{18}\text{O}_{\text{shell}}$  records can be used to detect precipitation events occurred on synoptic-scales. When applying this method, 12 negative shifts passed the 30th percentile of negative derivative values (Fig. 4f), which is treated as the threshold for identifying the significant excursions of the first derivative values (Wang et al., 2025). In other words, 12 precipitation events were detected. This is basically consistent with 11 precipitation events from instrumental data (Fig. 4h). However, it is challenging to conduct event-to-event correlations, because the natural system variability, such as spatial/temporal precipitation heterogeneity, may introduce environmental noise, and the  $\delta^{18}\text{O}_{\text{shell}}$  record micro-environmental conditions at sampling sites rather than meteorological data from the station 8 km away. For example, event 2 in Fig. 4f is probably not the same as the rain event numbered 2 in Fig. 4h. Moreover, there are 20 and 14 sub-samples for two dry periods, which correspond to 30 and 27 days, respectively (two yellow shaded intervals in Fig. 4). While 34 sub-samples were obtained for the wet period in-between, which represent 23 days (Fig. 4). This implies that the shell's growth rate varies with higher value in wet conditions, consistent with previous study (Wang et al., 2024a). Consequently, the discrepancy between the first derivative of  $\delta^{18}\text{O}_{\text{shell}}$  and instrumental data is not surprising.

We further conducted the first derivative analysis of the  $\delta^{18}\text{O}_{\text{shell}}$  of the three snail shells (0912-1, 0912-2, 0912-3), and the results showed that the variation pattern of reconstructed precipitation events is quite similar for shells formed in the same time period (Fig. S4). The suggested growth rates may not have large effect on the number and frequency of precipitation event. Furthermore, we compared our results with the recently published research at LW, ~130 km from SZS site (Wang et al., 2025). Encouragingly, the reconstructed weather-scale precipitation events from the SIMS  $\delta^{18}\text{O}_{\text{shell}}$  results by Wang et al. (2025) could be well compared with those from IRMS  $\delta^{18}\text{O}_{\text{shell}}$  in this work (Fig. S5).

Overall, the physiological traits of land snails make them typically sensitive to rainfall events. Thus, they are the ideal archives for studying high-resolution precipitation events. Our study demonstrates that the IRMS  $\delta^{18}\text{O}_{\text{shell}}$  has great potential for exploring the frequency of weather-scale precipitation changes, which is cheaper and more efficient compared with the SIMS  $\delta^{18}\text{O}_{\text{shell}}$  analysis. It will be highly beneficial to apply this method to fossil shells on the Chinese Loess Plateau, which could help us to understand the mechanisms of weather-scale precipitation events under different climatic types.

## 5. Conclusion

In this study, 625 high-resolution  $\delta^{18}\text{O}$  values were obtained from seven modern *C. fasciola* snails in the monsoon marginal zone by IRMS. The  $\delta^{18}\text{O}_{\text{shell}}$  records of different individuals show similar variation patterns and good reproducibility. The calculated growth rate of snails can reach ~543  $\mu\text{m}/\text{day}$ , which suggests that the high-resolution intra-shell samples at 500–800  $\mu\text{m}$  intervals could reach daily resolution by manual dental drill samplings. The reconstructed synoptic-scale precipitation frequency from the first derivative of the  $\delta^{18}\text{O}_{\text{shell}}$  profiles is in good agreement with the instrumental data. This suggests that this method has the potential to explore the weather-scale precipitation events from intra-shell  $\delta^{18}\text{O}_{\text{shell}}$  by IRMS in the monsoon marginal zone, which is superior to the SIMS analysis in terms of cost and efficiency. Therefore, it will be promising to unravel the information on synoptic-

scale precipitation events from fossils on the Chinese Loess Plateau, which will be helpful to deepen our understanding of their mechanisms under different climatic types.

## Credit author statement

**Qian Zhang:** Investigation, Data curation, Validation, Visualization, Formal analysis, Writing – original draft, Writing – review & editing. **Jibao Dong:** Conceptualization, Formal analysis, Data curation, Writing – review & editing, Funding acquisition. **Guozhen Wang:** Investigation, Methodology, Formal analysis, Writing – review & editing. **Fan Luo:** Data curation, Methodology. **Ya-na Jia:** Investigation, Formal analysis, Writing – review & editing. **Chengcheng Liu:** Resources, Writing – review & editing. **Xiulan Zong:** Formal analysis, Writing – review & editing. **Xiangzhong Li:** Formal analysis, Writing – review & editing. **John Dodson:** Writing – review & editing. **Hong Yan:** Funding acquisition, Project administration, Resources, Supervision, Writing – review & editing.

## Declaration of competing interest

The authors declare that they have no known competing financial interests or personal relationships that could have appeared to influence the work reported in this paper.

## Acknowledgments

This work was supported by the National Natural Science Foundation of China (NSFC) (42025304, 42377445), the National Key R&D Program of China (2023YFF0804804), the CAS Youth Interdisciplinary Team (2024000021), the Youth Innovation Promotion Association, Chinese Academy of Sciences. We also thank Haotian Yang, Jun Geng, Nanyu Zhao, Tao Han, Chengde Liang, and Heng Zhang from the Institute of Earth Environment CAS for their assistance with fieldwork.

## Appendix B. Supplementary data

Supplementary data to this article can be found online at <https://doi.org/10.1016/j.quascirev.2025.109582>.

## Data availability

Data are available through: [http://paleodata.iecas.cn/FrmDataInfo\\_EN.aspx?id=97be10e5-a9b4-4130-984c-d1a41be093c7](http://paleodata.iecas.cn/FrmDataInfo_EN.aspx?id=97be10e5-a9b4-4130-984c-d1a41be093c7).

## References

- Abell, P., Plug, I., 2000. The pleistocene/holocene transition in South Africa: evidence for the younger dryas event. *Global Planet. Change* 26 (1–3), 173–179. [https://doi.org/10.1016/s0921-8118\(00\)00042-4](https://doi.org/10.1016/s0921-8118(00)00042-4).
- An, Z., Clemens, S.C., Shen, J., Qiang, X., Jin, Z., Sun, Y., et al., 2011. Glacial-interglacial Indian summer monsoon dynamics. *Science* 333 (6043), 719–723. <https://doi.org/10.1126/science.1203752>.
- Añel, J., Fernández-González, M., Labandeira, X., López-Otero, X., De la Torre, L., 2017. Impact of cold waves and heat waves on the energy production sector. *Atmosphere* 8 (11), 209. <https://doi.org/10.3390/atmos8110209>.
- Balakrishnan, M., Yapp, C.J., 2004. Flux balance models for the oxygen and carbon isotope compositions of land snail shells. *Geochim. Cosmochim. Acta* 68 (9), 2007–2024. <https://doi.org/10.1016/j.gca.2003.10.027>.
- Bao, R., Sheng, X., Lu, H., Li, C., Luo, L., Shen, H., Wu, M., Ji, J., Chen, J., 2019. Stable carbon and oxygen isotopic composition of modern land snails along a precipitation gradient in the mid-latitude East Asian monsoon region of China. *Palaeogeogr. Palaeoclimatol. Palaeoecol.* 533, 109236. <https://doi.org/10.1016/j.palaeo.2019.109236>.
- Bao, R., Sheng, X., Li, C., Shen, H., Tan, L., Sun, L., Li, C., Peng, H., Luo, L., Wu, M., Lu, H., Ji, J., Chen, J., 2020. Effect of altitude on the stable carbon and oxygen isotopic compositions of land snails at the margin of the East Asian monsoon. *Geochim. Cosmochim. Acta* 273, 99–115. <https://doi.org/10.1016/j.gca.2020.01.029>.
- Barker, G.M., 2001. The Biology of Terrestrial Molluscs. Cromwell Press. <https://doi.org/10.1079/9780851993188.0000>. Trowbridge.

- Chen, F., Xu, Q., Chen, J., Birks, H.J.B., Liu, J., Zhang, S., Jin, L., An, C., Telford, R.J., Cao, X., Wang, Z., Zhang, X., Selvaraj, K., Lu, H., Li, Y., Zheng, Z., Wang, H., Zhou, A., Dong, G., Zhang, J., Huang, X., Bloemendal, J., Rao, Z., 2015. East Asian summer monsoon precipitation variability since the last deglaciation. *Sci. Rep.* 5 (1). <https://doi.org/10.1038/srep11186>.
- Chen, Y., Deng, H., Li, B., Li, Z., Xu, C., 2014. Abrupt change of temperature and precipitation extremes in the arid region of northwest China. *Quat. Int.* 336, 35–43. <https://doi.org/10.1016/j.quaint.2013.12.057>.
- Chen, D., Zhang, G., 2004. Fauna sinica (invertebrata vol. 37). In: *Mollusca: Gastropoda: Stylommatophora: Bradybaenidae*. Science Press, pp. 204–218 (in Chinese).
- Cheng, H., Edwards, R.L., Sinha, A., Spötl, C., Yi, L., Chen, S., et al., 2016. The Asian monsoon over the past 640,000 years and ice age terminations. *Nature* 534 (7609), 640–646. <https://doi.org/10.1038/nature18591>.
- Colonese, A.C., Zanchetta, G., Dotsika, E., Drysdale, R.N., Fallick, A.E., Grifoni Cremonesi, R., Manganelli, G., 2010. Early-middle Holocene land snail shell stable isotope record from Grotta di Latronico 3 (southern Italy). *J. Quat. Sci.* 25 (8), 1347–1359. <https://doi.org/10.1002/jqs.1429>.
- Cook, E.R., Anchukaitis, K.J., Buckley, B.M., D'Arrigo, R.D., Jacoby, G.C., Wright, W.E., 2010. Asian monsoon failure and megadrought during the last millennium. *Science* 328 (5977), 486–489. <https://doi.org/10.1126/science.1185188>.
- Dettman, D.L., Sawada, Y., Pickford, M., 2024. High resolution stable isotope ratios in modern African land snails: testing inferred environmental conditions. *Quat. Sci. Rev.* 344, 108943. <https://doi.org/10.1016/j.quascirev.2024.108943>.
- Donat, M.G., Angélil, O., Ukkola, A.M., 2019. Intensification of precipitation extremes in the world's humid and water-limited regions. *Environ. Res. Lett.* 14 (6), 065003. <https://doi.org/10.1088/1748-9326/ab1c8e>.
- Donat, M.G., Lowry, A.L., Alexander, L.V., O'Gorman, P.A., Maher, N., 2016. More extreme precipitation in the world's dry and wet regions. *Nat. Clim. Change* 6 (5), 508–513. <https://doi.org/10.1038/nclimate2941>.
- Dong, Yan, H., Zong, X., Wang, G., Liu, C., Xing, M., et al., 2022. Ultra-high resolution  $\delta^{18}\text{O}$  of land snail shell: a potential tool to reconstruct frequency and intensity of paleoprecipitation events. *Geochem. Cosmochim. Acta* 327, 21–33. <https://doi.org/10.1016/j.gca.2022.04.015>.
- Ghosh, P., Rangarajan, R., Thirumalai, K., Naggs, F., 2017. Extreme monsoon rainfall signatures preserved in the invasive terrestrial gastropod *lissachatina fulica*. *G-cubed* 18 (11), 3758–3770. <https://doi.org/10.1002/2017gc007041>.
- Goodfriend, G.A., 1992. The use of land snail shells in paleoenvironmental reconstruction. *Quat. Sci. Rev.* 11 (6), 665–685. [https://doi.org/10.1016/0277-3791\(92\)90076-k](https://doi.org/10.1016/0277-3791(92)90076-k).
- Goodfriend, G.A., Ellis, G.L., 2002. Stable carbon and oxygen isotopic variations in modern rabbitid land snail shells in the southern great plains, USA, and their relation to environment. *Geochem. Cosmochim. Acta* 66 (11), 1987–2002. [https://doi.org/10.1016/s0016-7037\(02\)00824-4](https://doi.org/10.1016/s0016-7037(02)00824-4).
- Goodfriend, G.A., Magaritz, M., Gat, J.R., 1989. Stable isotope composition of land snail body water and its relation to environmental waters and shell carbonate. *Geochem. Cosmochim. Acta* 53 (12), 3215–3221. [https://doi.org/10.1016/0016-7037\(89\)90102-6](https://doi.org/10.1016/0016-7037(89)90102-6).
- Hong, W., Fang, M., Zhu, X., Sun, Q., Zhang, L., Zhang, C., 2006. The occurrence, causes, and control of snails in vegetables in the hangzhou area. *Zhejiang Agricultural Sciences* (6), 683–685 (in Chinese).
- Kehrwald, N.M., McCoy, W.D., Thibault, J., Burns, S.J., Oches, E.A., 2010. Paleoclimatic implications of the spatial patterns of modern and LGM European land-snail shell  $\delta^{18}\text{O}$ . *Quaternary Research* 74 (1), 166–176. <https://doi.org/10.1016/j.yqres.2010.03.001>.
- Lécole, P., 1985. The oxygen isotope composition of landsnail shells as a climatic indicator: applications to hydrogeology and paleoclimatology. *Chem. Geol. Isot. Geosci.* 58 (1–2), 157–181. [https://doi.org/10.1016/0168-9622\(85\)90036-3](https://doi.org/10.1016/0168-9622(85)90036-3).
- Lehmann, J., Coumou, D., Frieler, K., 2015. Increased record-breaking precipitation events under global warming. *Clim. Change* 132 (4), 501–515. <https://doi.org/10.1007/s10584-015-1434-y>.
- Leng, M.J., Heaton, T.H.E., Lamb, H.F., Naggs, F., 1998. Carbon and oxygen isotope variations within the shell of an African land snail (*Limicolaria kambeul chudeaui germaini*): a high-resolution record of climate seasonality? *Holocene* 8 (4), 407–412. <https://doi.org/10.1191/095968398669296159>.
- Lesk, C., Rowhani, P., Ramankutty, N., 2016. Influence of extreme weather disasters on global crop production. *Nature* 529 (7584), 84–87. <https://doi.org/10.1038/nature16467>.
- Li, F., Rousseau, D.-D., Wu, N., Hao, Q., Pei, Y., 2008. Late Neogene evolution of the East Asian monsoon revealed by terrestrial mollusk record in Western Chinese loess Plateau: from winter to summer dominated sub-regime. *Earth Planet Sci. Lett.* 274 (3–4), 439–447. <https://doi.org/10.1016/j.epsl.2008.07.038>.
- Li, F., Wu, N., Dong, Y., Zhang, D., Zhang, Y., Huang, L., et al., 2021. Land-snail eggs as a proxy of abrupt climatic cooling events during the reproductive season. *Science Bulletin* 66 (13), 1274–1277. <https://doi.org/10.1016/j.scib.2021.02.017>.
- Li, Q., Dong, J., Yan, H., Huang, H., Zong, X., Wang, G., et al., 2024. High-resolution intrashell oxygen isotope studies of *cathaca fasciola* and *Bradybaena ravidula* land snails and their environmental implications. *Geophys. Res. Lett.* 51 (6). <https://doi.org/10.1029/2023gl107835>.
- Liu, T., 1985. Loess and the Environment. China Ocean Press, Beijing (in Chinese).
- Liu, Z., Gu, Z., Xu, B., Wu, N., 2006. Effects of summer monsoon precipitation on the oxygen isotope composition of carbonate shells of extant snails on the loess Plateau. *Quat. Sci.* 26 (4), 643–648 (in Chinese).
- Liu, T., Ding, Z., 1998. Chinese loess and the paleomonsoon. *Annu. Rev. Earth Planet Sci.* 26 (1), 111–145. <https://doi.org/10.1146/annurev.earth.26.1.111>.
- Magaritz, M., Heller, J., 1980. A desert migration indicator — oxygen isotopic composition of land snail shells. *Palaeogeogr. Palaeoclimatol. Palaeoecol.* 32, 153–162. [https://doi.org/10.1016/0031-0182\(80\)90038-3](https://doi.org/10.1016/0031-0182(80)90038-3).
- Meehl, G.A., Karl, T., Easterling, D.R., Changnon, S., Pielke, R., Changnon, D., et al., 2000. An introduction to trends in extreme weather and climate events: observations, socioeconomic impacts, terrestrial ecological impacts, and model projections\*. *Bull. Am. Meteorol. Soc.* 81 (3), 413–416. [https://doi.org/10.1175/1520-0477\(2000\)081<0413:aitte>2.3.co;2](https://doi.org/10.1175/1520-0477(2000)081<0413:aitte>2.3.co;2).
- Mei, L., 2016. Analysis of the causes of occurrence and control strategies of vegetable snails. *Seed Sci. Technol.* 34 (11), 110–111 (in Chinese).
- Nield, C.B., Yanes, Y., Pigati, J.S., Rech, J.A., von Proschwitz, T., Nekola, J.C., 2022. Oxygen isotopes of land snail shells in high latitude regions. *Quat. Sci. Rev.* 279, 107382. <https://doi.org/10.1016/j.quascirev.2022.107382>.
- Oosterhoff, L.M., 1977. Variation in growth rate as an ecological factor in the landsnail *Cepaea nemoralis* (L.). *Neth. J. Zool.* 27 (1), 1–132. <https://doi.org/10.1163/002829677x00072>.
- Prendergast, A.L., Stevens, R.E., Barker, G., O'Connell, T.C., 2015. Oxygen isotope signatures from land snail (*helix Melanostoma*) shells and body fluid: proxies for reconstructing mediterranean and North African rainfall. *Chem. Geol.* 409, 87–98. <https://doi.org/10.1016/j.chemgeo.2015.05.014>.
- Rangarajan, R., Ghosh, P., Naggs, F., 2013. Seasonal variability of rainfall recorded in growth bands of the giant African land snail *lissachatina fulica* (Bowdich) from India. *Chem. Geol.* 357, 223–230. <https://doi.org/10.1016/j.chemgeo.2013.08.015>.
- Rech, J.A., Pigati, J.S., Springer, K.B., Bosch, S., Nekola, J.C., Yanes, Y., 2021. Oxygen isotopes in terrestrial gastropod shells track Quaternary climate change in the American southwest. *Quaternary Research* 104, 43–53. <https://doi.org/10.1017/qua.2021.18>.
- Rousseau, D.-D., Wu, N., 1997. A new molluscan record of the monsoon variability over the past 130 000 yr in the luochuan loess sequence, China. *Geology* 25 (3), 275. [https://doi.org/10.1130/0091-7613\(1997\)025<0275:amrrot>2.3.co;2](https://doi.org/10.1130/0091-7613(1997)025<0275:amrrot>2.3.co;2), 275.
- Thakur, S., Kumari, R., 1998. Seasonal behaviour of giant African snail *Achatina fulica* in Bihar. *J. Ecotoxicol. Environ. Monit.* 8, 153–160.
- Trenberth, K., 1999. Conceptual framework for changes of extremes of the hydrological cycle with climate change. *Clim. Change* 42, 327–339. <https://doi.org/10.1023/a:1005488920935>.
- Ummenhofer, C.C., Meehl, G.A., 2017. Extreme weather and climate events with ecological relevance: a review. *Phil. Trans. Biol. Sci.* 372 (1723), 20160135. <https://doi.org/10.1098/rstb.2016.0135>.
- Upatham, E.S., Kruratracue, M., Baidikul, V., 1988. Cultivation of the giant African snail. *Achatina fulica* 14, 25–40.
- Wang, G., Dong, J., Han, T., Liu, C., Luo, F., Yang, H., et al., 2024a. Quantitative reconstruction of a single super rainstorm using daily resolved  $\delta^{18}\text{O}$  of land snail shells. *Science Bulletin* 69 (14), 2281–2288. <https://doi.org/10.1016/j.scib.2024.04.037>.
- Wang, G., Dong, J., Zhang, Q., He, S., Liu, C., Luo, F., et al., 2025. Frequency of synoptic-scale precipitation events recorded by daily resolved  $\delta^{18}\text{O}$  of Land Snail Shells. *Geophys. Res. Lett.* 52 (2). <https://doi.org/10.1029/2024gl112536>.
- Wang, M., Wang, X., Dettman, D.L., Wang, Q., Wu, D., Liu, W., et al., 2024b. Stable carbon isotope composition of land snail shells in westerlies Asia and monsoonal Asia: paleoclimate implications. *Quat. Sci. Rev.* 327, 108505. <https://doi.org/10.1016/j.quascirev.2024.108505>.
- Wang, X., Cui, L., Zhai, J., Ding, Z., 2016. Stable and clumped isotopes in shell carbonates of land snails *cathaica* sp. and *bradybaena* sp. in north China and implications for ecophysiological characteristics and paleoclimate studies. *G-cubed* 17 (1), 219–231. <https://doi.org/10.1002/2015gc006182>.
- Wang, X., Dettman, D.L., Wang, M., Zhang, J., Saito, Y., Quade, J., et al., 2020. Seasonal wet-dry variability of the Asian monsoon since the middle Pleistocene. *Quat. Sci. Rev.* 247, 106568. <https://doi.org/10.1016/j.quascirev.2020.106568>.
- Wang, X., Zhai, J., Cui, L., Zhang, S., Ding, Z., 2019. Stable carbon and oxygen isotopes in shell carbonates of modern land snails in China and their relation to environment variables. *J. Geophys. Res.: Biogeosciences* 124 (11), 3356–3376. <https://doi.org/10.1029/2019jg005255>.
- Wu, N., Denis-Didier, R., Liu, T., 1998. Climatic instability in the loess snail fossil record during the late last glacial period. *Chin. Sci. Bull.* 15, 1654–1658 (in Chinese).
- Wu, N., Pei, Y., Lu, H., Denis-Didier, R., 2001. Differences in winter and summer monsoon cycles in the loess Plateau over the past 350,000 years—evidence from terrestrial snail fossils. *Quat. Sci. (6)*, 540–550 (in Chinese).
- Wu, N., Li, F., Rousseau, D.-D., 2018. Terrestrial mollusk records from Chinese loess sequences and changes in the East Asian monsoonal environment. *J. Asian Earth Sci.* 155, 35–48. <https://doi.org/10.1016/j.jseas.2017.11.003>.
- Xu, W., Wang, R., Wu, C., Mao, Y., Ge, Y., Tang, G., 2002. The occurrence characteristics and control strategies of snails in farmlands of the Jiangsu coastal area. *Entomological Journal of East China* (2), 63–69 (in Chinese).
- Yan, H., Liu, C., An, Z., Yang, W., Yang, Y., Huang, P., et al., 2020. Extreme weather events recorded by daily to hourly resolution biogeochemical proxies of marine giant clam shells. *Proc. Natl. Acad. Sci.* 117 (13), 7038–7043. <https://doi.org/10.1073/pnas.1916784117>.
- Yanes, Y., Graves, G.R., Romanek, C.S., 2018. Stable isotope ecology ( $\delta^{18}\text{O}$ ,  $\delta^{13}\text{C}$ ,  $\delta^{15}\text{N}$ ) of modern land snails along an altitudinal gradient in southern Appalachian Mountains, USA. *Palaeogeogr. Palaeoclimatol. Palaeoecol.* 492, 92–103. <https://doi.org/10.1016/j.palaeo.2017.12.015>.
- Yanes, Y., Al-Qattan, N.M., Rech, J.A., Pigati, J.S., Dodd, J.P., Nekola, J.C., 2019. Overview of the oxygen isotope systematics of land snails from North America. *Quaternary Research* 91 (1), 329–344. <https://doi.org/10.1017/qua.2018.79>.
- Yanes, Y., Izeta, A.D., Cattáneo, R., Costa, T., Gordillo, S., 2014. Holocene (~4.5–1.7 cal. kyr BP) paleoenvironmental conditions in central Argentina inferred from entire-

- shell and intra-shell stable isotope composition of terrestrial gastropods. *Holocene* 24 (10), 1193–1205. <https://doi.org/10.1177/0959683614540959>.
- Yapp, C.J., 1979. Oxygen and carbon isotope measurements of land snail shell carbonate. *Geochem. Cosmochim. Acta* 43 (4), 629–635. [https://doi.org/10.1016/0016-7037\(79\)90170-4](https://doi.org/10.1016/0016-7037(79)90170-4).
- Zachos, J., Pagani, M., Sloan, L., Thomas, E., Billups, K., 2001. Trends, rhythms, and aberrations in global climate 65 Ma to present. *Science* 292 (5517), 686–693. <https://doi.org/10.1126/science.1059412>.
- Zanchetta, G., Leone, G., Fallick, A.E., Bonadonna, F.P., 2005. Oxygen isotope composition of living land snail shells: data from Italy. *Palaeogeogr. Palaeoclimatol. Palaeoecol.* 223 (1–2), 20–33. <https://doi.org/10.1016/j.palaeo.2005.03.024>.
- Zong, X., Dong, J., Song, Y., Yan, H., Xing, M., Liu, W., et al., 2023. Precipitation  $\delta^{18}\text{O}$  paced the seasonal  $\delta^{18}\text{O}$  variations of terrestrial snail body water and shells in the East Asian monsoon region. *Quat. Sci. Rev.* 317, 108290. <https://doi.org/10.1016/j.quascirev.2023.108290>.